

AN INVESTIGATION OF THE OPTICAL PROPERTIES OF NANOCRYSTAL
SUPERPARTICLES

Sai Murali Karthik Putcha

A THESIS

in

Materials Science and Engineering

Presented to the Faculties of the University of Pennsylvania

in

Partial Fulfillment of the Requirements for the

Degree of Master of Science in Engineering

2023

*Professor Christopher B. Murray,
Richard Perry University Professor of Chemistry and Materials Science and Engineering
Supervisor of Thesis*

*Professor Mahadevan Khantha,
Director, Master's Program in Materials Science and Engineering*

AN INVESTIGATION OF THE OPTICAL PROPERTIES OF NANOCRYSTAL
SUPERPARTICLES

© COPYRIGHT

2023

Sai Murali Karthik Putcha

This work is licensed under the
Creative Commons Attribution
NonCommercial-ShareAlike 3.0
License

To view a copy of this license, visit

<http://creativecommons.org/licenses/by-nc-sa/3.0/>

ACKNOWLEDGEMENT

I would like to wholeheartedly thank Professor Christopher B. Murray for allowing me to work in his lab and all the Murray group members for helping me along this journey.

TABLE OF CONTENTS

| | |
|--|-----|
| ACKNOWLEDGEMENT | ii |
| LIST OF TABLES | v |
| LIST OF ILLUSTRATIONS | vii |
| CHAPTER 1 : NANOCRYSTALS | 1 |
| 1.1 Introduction | 1 |
| 1.2 Quantum Confinement | 1 |
| 1.3 Surface and trap states | 3 |
| 1.4 Light generation in quantum dots | 4 |
| 1.5 Absorption and photoluminescence (PL) | 4 |
| 1.6 Effect of surface passivation on optical properties | 8 |
| CHAPTER 2 : THE COLLECTIVE OPTICAL PROPERTIES OF CLUSTERS OF NANOCRYSTALS | 10 |
| 2.1 Förster Resonance Energy Transfer (F.R.E.T.) | 10 |
| 2.2 Whispering Gallery Modes | 11 |
| 2.3 Lasing | 12 |
| CHAPTER 3 : SYNTHESIS AND CHARACTERIZATION OF NANOCRYSTAL SUPERPARTICLES | 14 |
| 3.1 Microfluidic synthesis of nanocrystal superparticles | 14 |
| 3.2 Measuring the optical properties of the superparticles | 15 |
| CHAPTER 4 : RESULTS AND DISCUSSION | 16 |
| 4.1 Dueling Peaks | 16 |
| 4.2 CdTe superparticles | 16 |

| | |
|--|----|
| 4.3 CdSe superparticles | 17 |
| 4.4 CdSe + CdSe/CdS superparticles | 20 |
| CHAPTER 5 : FURTHER WORK | 27 |
| 5.1 Solving the mystery of the dueling peaks | 27 |
| 5.2 Solution-Processed twisted light laser | 28 |
| APPENDIX | 29 |
| BIBLIOGRAPHY | 29 |

LIST OF TABLES

TABLE 1 : Parameters used in the making of superparticles 15

TABLE 2 : Parameters used in measuring the optical properties of superparticles 15

LIST OF ILLUSTRATIONS

| | |
|---|----|
| FIGURE 1 : Quantum Confinement increases the band gap | 2 |
| FIGURE 2 : Band gap versus size of quantum dots. | 3 |
| FIGURE 3 : CdSe Absorption Spectra and Transition States | 5 |
| FIGURE 4 : Absorption and photoluminescence spectra, and Stokes Shift . . . | 6 |
| FIGURE 5 : Trap Emission in PL (Red arrow) and Energy states corresponding to trap states | 6 |
| FIGURE 6 : Size dependence on absorbance and photoluminescence spectra . . | 7 |
| FIGURE 7 : Fitting absorption spectrum with Gaussian waveforms to confirm broadening | 8 |
| FIGURE 8 : Effects of ligands with different number of carbon atoms on the optical properties of NCs(13) | 9 |
| FIGURE 9 : Effect of inorganic surface passivant on PL of CdSe NCs | 9 |
| FIGURE 10 : Effect of FRET on PL and exciton lifetimes | 11 |
| FIGURE 11 : "Crosstalk" between absorption of one NC and PL of another NC. | 11 |
| FIGURE 12 : Redshift is seen in PL of perovskite NC superclusters. The redshift depends on the arrangement of NCs. | 12 |
| FIGURE 13 : | 13 |
| FIGURE 14 : Lasing observed in NC superparticles(20) | 13 |
| FIGURE 15 : Dueling Peaks mountains in the video game The Legend of Zelda: Breath of the Wild | 16 |
| FIGURE 16 : CdTe superparticles optical micrographs | 17 |
| FIGURE 17 : PL and Absorbance Spectra of CdSe [550nm] NCs. | 18 |
| FIGURE 18 : CdSe [550nm] superparticles optical micrographs and corresponding PL spectra at various locations on the substrate. | 19 |

| | |
|---|----|
| FIGURE 19 : PL and Absorbance Spectra of CdSe [536nm] NCs. | 21 |
| FIGURE 20 : CdSe [536nm] superparticles optical micrographs and corresponding PL spectra at various locations on the substrate. The second peak re-emerges as well as a significant population of red-emitting SPs. | 22 |
| FIGURE 21 : PL and Absorbance Spectra of CdSe/CdS core-shell NCs used to make SPs. | 23 |
| FIGURE 22 : CdSe _{0.25} CdSe/CdS _{0.75} superparticles optical micrographs and corresponding PL spectra at various locations on the substrate. Two peaks are observed. | 24 |
| FIGURE 23 : CdSe _{0.5} CdSe/CdS _{0.5} superparticles optical micrographs and corresponding PL spectra at various locations on the substrate. Two peaks are observed. | 26 |
| FIGURE 24 : | 28 |

CHAPTER 1 : NANOCRYSTALS

1.1. Introduction

Humans were always fascinated by light since ancient times. Early humans were curious about what the sparkles in the night sky are and what the large white ball in the sky during the day is. Light generation and control is not an avenue of exploration only meant to quench curiosity, it can have many practical uses as well. As humanity progressed, we learned to generate light and control it at will. This ability helped us eliminate the limitations of darkness at night and allows us to communicate with others across the world. It can also be used for entertainment, in the form of smartphone and television displays, and bright floodlights that give life to a music concert, for example. There are many approaches to generating and controlling light. One leading approach is to use nanometer-sized crystals of semiconducting material. They are a great way to control the emission of light that can be tuned to a particular frequency simply by changing the size of these crystals. This versatility allows for building color-accurate television displays and even lasers.

1.2. Quantum Confinement

Nanocrystals are nanometer-sized crystals of semiconducting solid matter. Solid matter is made of atoms that are held together by electrons. In a semiconducting material, electrons of a high enough energy are free to move about in the crystal and when they lose this energy, they emit a photon of light of a frequency characteristic to the material. In the case of a nanocrystal, this frequency also depends on the size and shape of the crystal(12). The dependence on size for quantum dots which are spherically symmetrical nanocrystals is shown in the figure given below. As the diameter increases, the band gap gets smaller and smaller due to the lesser extent of confinement of electrons. In this thesis, we will focus on spherically-symmetric nanocrystals called quantum dots (QDs).

To describe the behavior of electrons in a crystal, we often use the time-independent

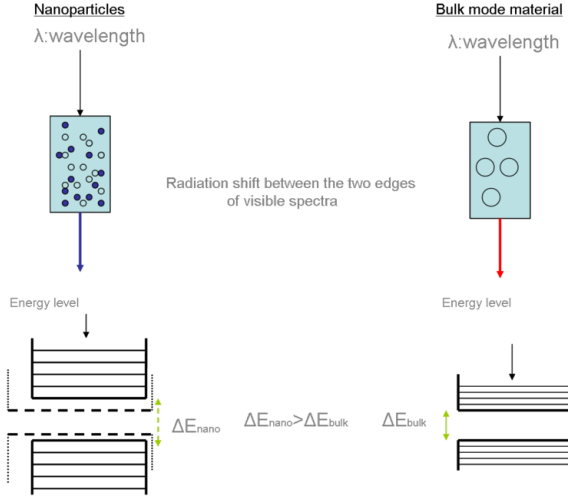


Figure 1: Quantum Confinement increases the band gap

Schrödinger equation:

$$-\frac{\hbar^2}{2m^*} \nabla^2 \psi(x, y, z) + \hat{V}(x, y, z)\psi(x, y, z) = E\psi(x, y, z)$$

Where m^* is the effective mass of the electron in the material, $\psi(x, y, z)$ is the wave function of the electron (the modulus of which describes the electron's probability of existing at [x, y, z]), $\hat{V}(x, y, z)$ is the potential experienced by an electron at [x, y, z], and E is the total energy of the electron. This equation basically expresses the conservation of energy of the electron in the crystal. In a quantum dot, the potential would be a constant throughout the nanocrystal and goes to a very large value outside the dot, thus it would look like a potential well(12). The resulting energy band structure looks like that given in Figure 1 (3)(23).

Some common geometries of nanocrystals(9) are dots, rods, platelets, etc. The geometry and size of the crystals decide the boundary conditions of the electron's wavefunction and also change the values of allowed energy states of the electrons within the crystal, as given by the Schrodinger equation. In particular, there is a large difference between the energy of each band of allowed states compared to that within a band. This difference is characteristic of the material and geometry and photons of this energy are emitted from the nanocrystal¹.

¹We will see later in this chapter that there will be a broadening in the spectrum of emitted photons due

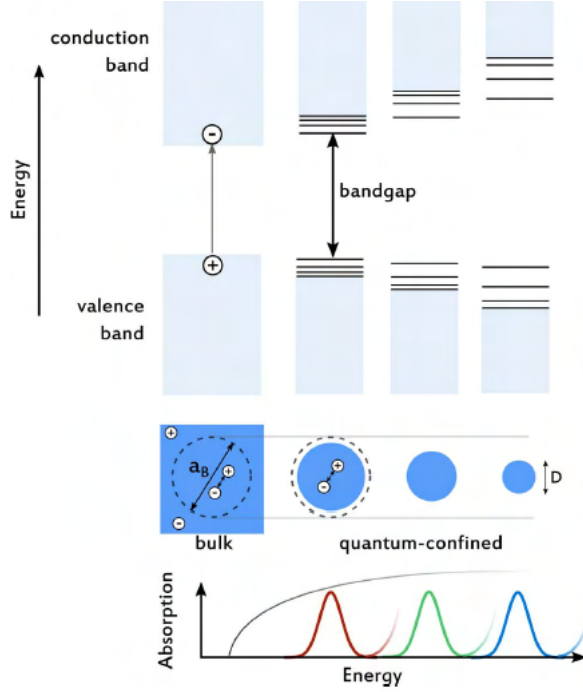


Figure 2: Band gap versus size of quantum dots.

Size affects the size of the band gap as given in the following Figure 2.

1.3. Surface and trap states

After solving the Schrödinger equation for electrons in the quantum dot, the solution wave function is wave-like throughout the inner core of the QD. For these electrons, near the surface of the quantum dot, the wave function tends to exponentially decay due to a phenomenon called quantum tunneling. For electrons near the surface, however, the wave function decays exponentially in both directions, while maintaining a wave-like character towards the core. This causes a change in the allowed energy states of the electrons near the surface and leads to the formation of sub-bands. These energy states are called **surface states**(6)(8)(22).

It is also possible for certain structural defects to be present on the surface or within the QD. This will lead to further change in the allowed energy states near the defects() figure

to small size discrepancies and thermal effects

of defective QDs. It might also happen that multiple QDs polymerize and cause changes to the wavefunction of the electron by lowering confinement (1). The new states formed by the above reasons are called **trap states**. However, there still might be reasons for some of these states to emerge that have been unaccounted for even in current literature (22).

1.4. Light generation in quantum dots

Light is generated from material in two possible ways: Stimulated emission or spontaneous emission. We will focus on stimulated emission in this work. Stimulated emission occurs when an electron gets excited to a higher energy level by absorbing a photon and releases a photon when it relaxes back to the lower energy level. When an electron gains enough energy to get unbound from an atom it leaves in its original place a vacancy called a "hole." This hole can be modeled as being a particle with the opposite charge as the electron. The hole attracts the electron and the electron-hole pair is called an **exciton** (exciton image). The exciton behaves like Bohr's Hydrogen atom (24) and a characteristic Bohr radius can be defined for the exciton. A photon will be emitted when the electron recombines with the hole. In quantum dots, the Bohr radius is usually larger than the dot itself, which greatly increases the probability of electron-hole recombination. This is one reason for the superior optical properties of QDs relative to their bulk counterparts.

1.5. Absorption and photoluminescence (PL)

1.5.1. *Absorption*

Photons with energy lower than the band gap of the QD will not result in excitation and will be converted to lattice vibrations called phonons². Photons with energy higher than band gap may result in different electron excitations and this can be seen when we measure an **Absorption Spectrum** of our nanocrystal sample. An example absorption spectrum

²Unless there is an ultrafast multiphoton excitation which would lead to higher harmonic generation (24). But in this work, we focus on single photon excitations

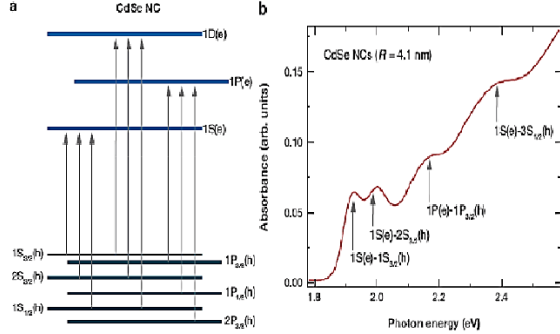


Figure 3: CdSe Absorption Spectra and Transition States

for a CdSe sample is shown in Figure 3 () .

1.5.2. Photoluminescence (PL)

Despite having many possible transitions in the QD, usually photons are emitted only from the 1S transition (as shown in the above figure for transition states). Electrons excited to higher energy states usually non-radiatively relax to the 1S conduction band edge. The energy of these relaxations is usually converted to phonons. To see the spectrum of emitted photons we can observe the **photoluminescence (PL) spectrum** of our sample. While measuring the PL of the sample, we excite the electrons in the sample with light of energy much higher than the 1S transition of the sample (we typically excite in the UV region), and measure what comes out on the other end of the sample. Photoluminescence refers to the fact that the light coming out of the sample is caused by irradiation by light. It can also be caused by an electric field, which is called electroluminescence. The general term for light coming out of a sample is fluorescence. The peak that we observe will have a shift in energy relative to the 1S transition that we observed in the absorption spectrum. This shift is called the **Stokes shift**. The resulting PL spectrum looks as shown in Figure 4, as well as the Stokes shift(1):

Trap emission

While the 1S transition can be the most prominent peak in the PL spectrum, when the size of the NC becomes too small, the surface area increases dramatically relative to the volume, thus causing an abundance of surface and trap states. This will cause a broad secondary

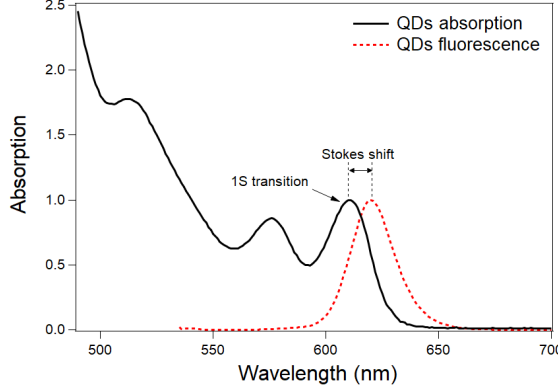


Figure 4: Absorption and photoluminescence spectra, and Stokes Shift

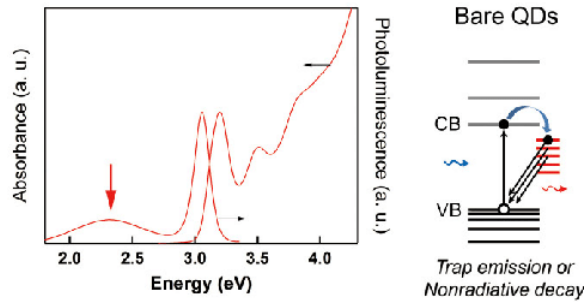


Figure 5: Trap Emission in PL (Red arrow) and Energy states corresponding to trap states

peak to emerge in the PL spectrum which is usually helpful in white light emission. The trap emission peak looks like as shown in Figure 5, highlighted by the red arrow(17):

Size dependence on Absorption and PL spectra

As we reduce the size of the QDs, the band gap energy increases which leads to a shift in the peak positions for both absorption and PL as shown in Figure 6(5)

1.5.3. Peak Broadening

It can be seen in the above spectra that the absorption and PL are not a sharp delta function (4)-like peak, but rather looks like a distribution. This broadening can occur due to multiple factors, but the prominent are size distribution broadening, confinement broadening, and Doppler broadening.

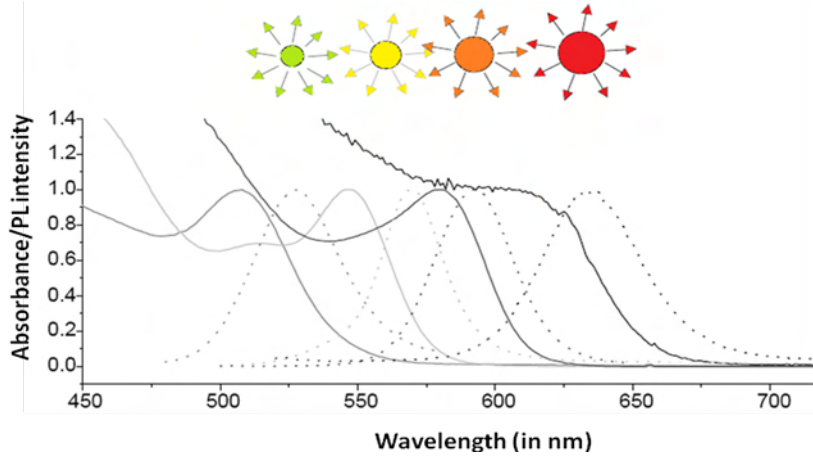


Figure 6: Size dependence on absorbance and photoluminescence spectra

Inhomogeneous Broadening

The transition states shown in the above figure are for NCs of a given size. In reality, it is difficult to synthesize purely monodisperse QDs and there will always be a distribution of sizes that leads to a distribution in the transition state energies. This is called **Inhomogeneous Broadening** (IHB) and is Gaussian in nature:

$$I^{\text{IHB}}(\nu) = \frac{1}{\sqrt{2\pi}\xi_0} \exp \left[-\frac{(\nu - \nu^{\text{IHB}}_0)^2}{\xi_0^2} \right]$$

, where ν^{IHB}_0 is the frequency of the most probable transition, i.e. that corresponding to the most common NC size, and ξ_0 is the FWHM of the peak due to IHB(7).

Homogeneous Broadening

Samples of the exact same size can also show broadening. This is called **Homogeneous Broadening** (HB) and occurs due to there being a phase difference in the emitted photons and also due to thermal effects. this is Lorentzian in nature:

$$I^{\text{HB}}(\nu^{\text{HB}}_i - \nu^{\text{HB}}_j) = \frac{1}{\pi} \frac{\Gamma^{\text{HB}}/2}{(\nu^{\text{HB}}_i - \nu^{\text{HB}}_j)^2 + (\Gamma^{\text{HB}}/2)^2}$$

, where ν^{HB}_i and ν^{HB}_j are the characteristic transition frequencies for i^{th} and j^{th} sized NCs respectively and Γ^{HB} is the FWHM of the inhomogenous broadening(7).

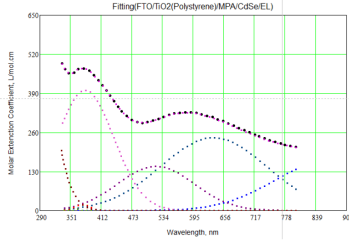


Figure 7: Fitting absorption spectrum with Gaussian waveforms to confirm broadening

So the actual spectrum would be a linear combination of these two broadening effects which looks as shown in the fitted absorption spectra shown in Figure 7

1.6. Effect of surface passivation on optical properties

When we want a higher energy fluorescence peak, we can reduce the size of our NCs. However, an unintended consequence of this is the increase of surface trap states that give rise to a secondary peak. Also, as QDs are in solution, we do not want them to coalesce and break the quantum confinement. To prevent these from happening, we can passivate the surface of the QDs. There are two ways we can do this:

1.6.1. Organic passivants (ligands)

To prevent QDs from coalescing and to make sure that there is charge neutrality on the surface of the QDs, we can passivate the surface with carbon chains called ligands. But these ligands also have an effect on the optical properties of our sample. One reason is that they come in the way of the light that exits the QD, but another reason is that they help tune the trap states on the surface of the QD. The number of carbon atoms decides the optical properties like PL peak position and refractive index. This can be seen in Figure 8(15)(13):

1.6.2. Inorganic passivants (Core-shell heterostructures)

Another way to eliminate surface trap states is to passivate by an inorganic layer, thus forming a core-shell heterostructure. However, this also results in a further shift in the PL peak. An example of the effect of passivating CdSe NCs with ZnS is shown in Figure 9(10).

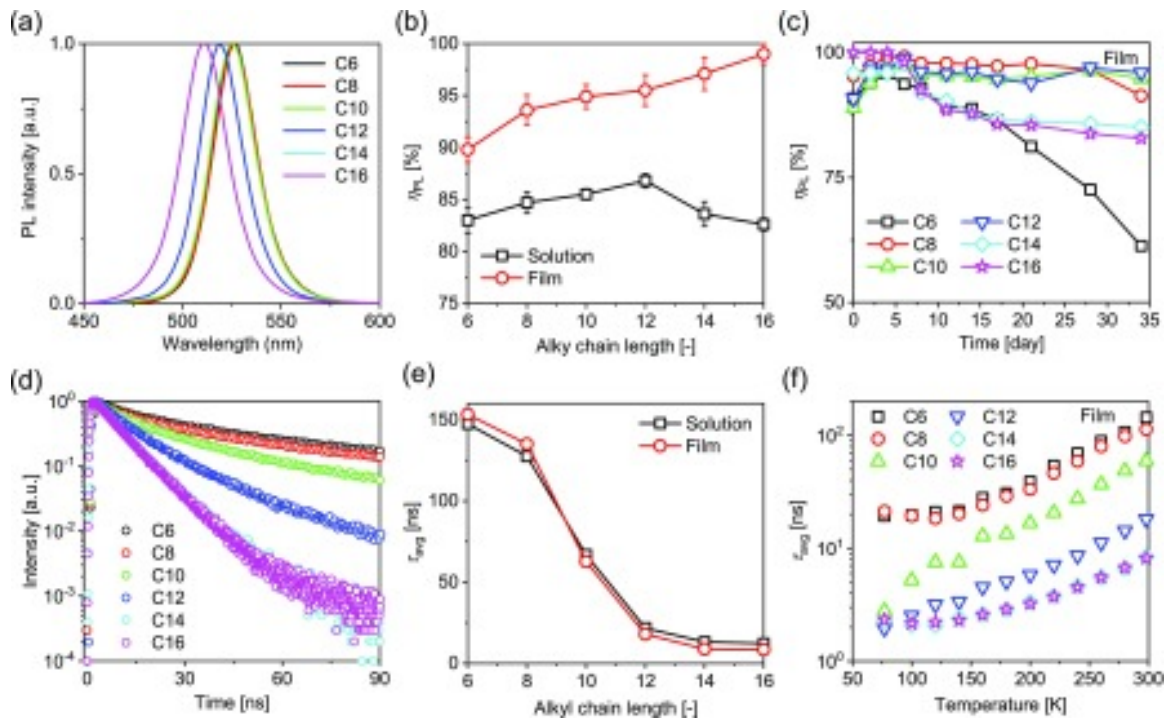


Figure 8: Effects of ligands with different number of carbon atoms on the optical properties of NCs(13)

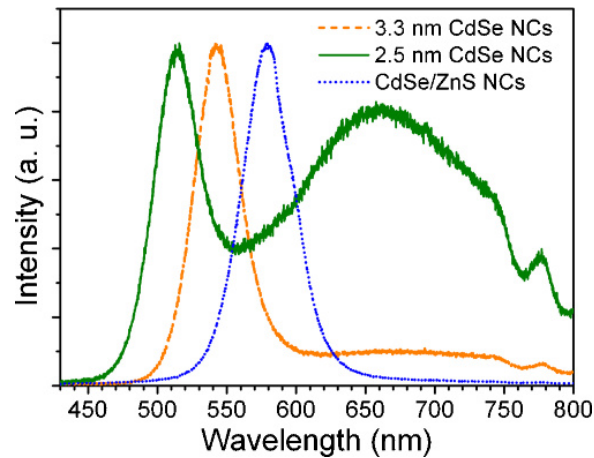


Figure 9: Effect of inorganic surface passivant on PL of CdSe NCs

CHAPTER 2 : THE COLLECTIVE OPTICAL PROPERTIES OF CLUSTERS OF NANOCRYSTALS

While nanocrystals have unique properties on their own that differ from that of their bulk counterparts due to quantum confinement, clustering nanocrystals give rise to many more novel, useful and interesting phenomena due to the interactions between the NCs. Taking advantage of these interactions would require strategically fabricating superclusters out of NCs with specific geometries tailored to the properties we would like to obtain. Before that, it is paramount to understand what these interactions are and what properties do they give rise to. The following sections are an attempt at laying out this understanding for a few mechanisms.

2.1. Förster Resonance Energy Transfer (F.R.E.T.)

When nanocrystals are close to each other, the excitons in one nanocrystal couple with that in another close-by NC. This occurs when the NCs are typically separated by about 2-10nm, and the phenomenon is called Förster Resonance Energy Transfer (F.R.E.T.). The FRET efficiency is given by (11):

$$\eta^{\text{FRET}} = \frac{nR_0^6}{nR_0^6 + r^6}$$

, where R_0 is the Förster distance, n is the average number of acceptor NCs interacting with a donor NC, and r is the spacing between a donor-acceptor (D-A) pair. As r decreases, η^{FRET} goes up and the interaction becomes stronger, thereby lowering exciton lifetimes, and redshifting the PL peak¹. This can be seen in Figure 10

This occurs because there is a "cross-talk" between the emission of the donor species and absorption of the acceptor species, which is illustrated in Figure 11(11).

The geometry and dimensionality of the arrangement of the NCs changes the optical

¹For CdSe, a redshift of only 35-50meV has been observed(21)

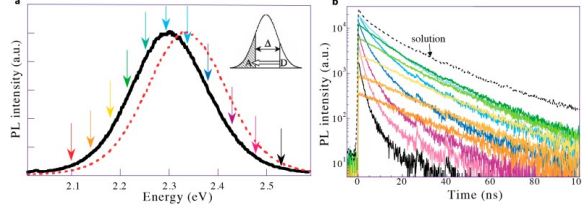


Figure 10: Effect of FRET on PL and exciton lifetimes

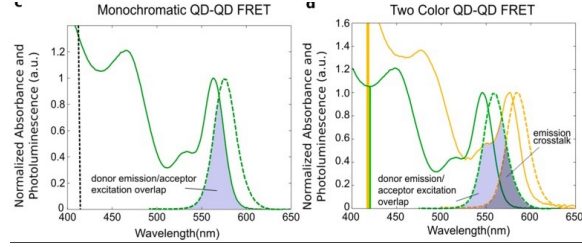


Figure 11: "Crosstalk" between absorption of one NC and PL of another NC.

properties(16). This work will focus more on the 3D spherical randomly arranged NCs in the form of superparticles (SPs). The effect of arrangement on properties are given in Figure 12.

2.2. Whispering Gallery Modes

When a resonator with at least an axis of symmetry is excited at its resonance frequency, it gives rise to standing waves of light called whispering gallery modes (WGM), on the surface of the resonator. The standing waves have multiple modes depending on the geometry of the resonator. For WGM to exist in the visible region of the electromagnetic spectrum, the resonators have to be several microns in size. Light-emitting NCs in the configuration of a micron-sized spherical superparticle is an interesting way to get WGM resonance in the visible region. CdSe NCs emit in visible as well, especially when trap states are enhanced to give broad, white trap emission. The WGM resonances in a CdSe/CdS core-shell SP can be seen in the below figure. The WGM resonances tend to overlap with the PL of the NCs used to make the SPs.

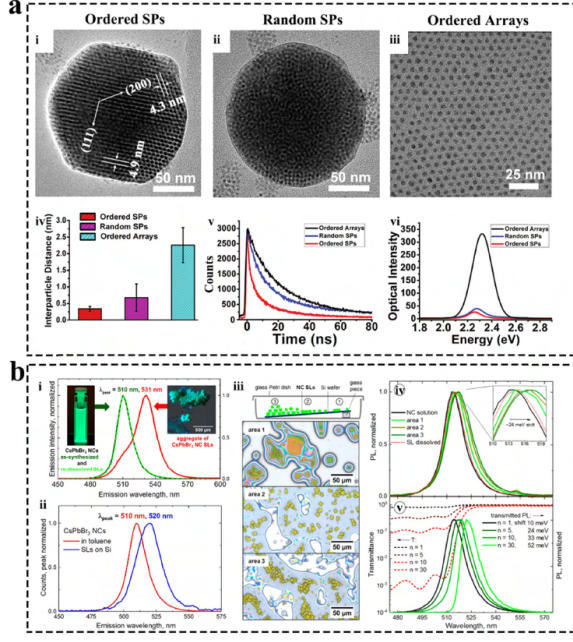
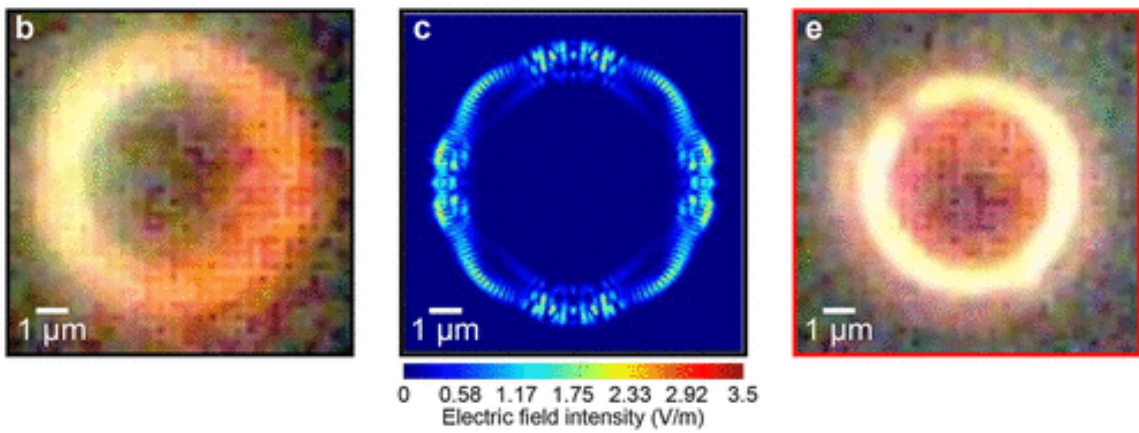


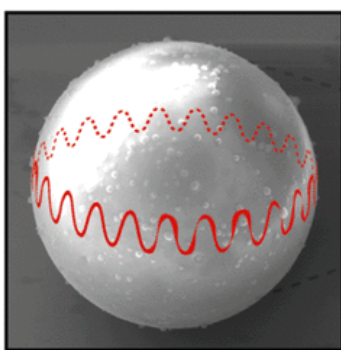
Figure 12: Redshift is seen in PL of perovskite NC superclusters. The redshift depends on the arrangement of NCs.

2.3. Lasing

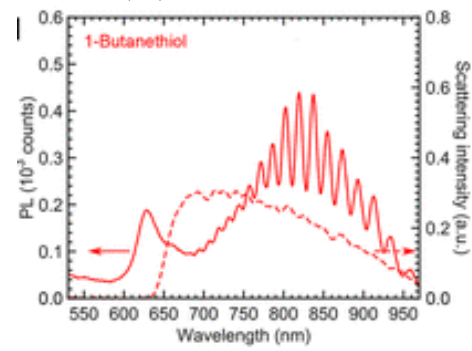
WGM resonances are very narrow compared to the broadening of PL in NCs and are similar to that of a laser. Added to that, the timescale of WGM resonances is much lower than that of exciton relaxation in QDs. This can be taken advantage of to generate lasing from the superparticles. Lasing peaks can be seen in Figure 14.



(a) WGM observed in CdSe/CdS NC SPs(18)



(b) WGM depicted on a spherical microresonator(20)



(c) WGM resonances showing up as peaks within the trap emission region of PL of CdSe/CdS(18)

Figure 13

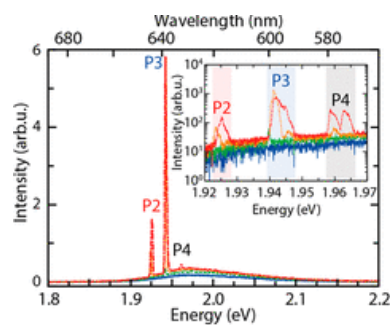


Figure 14: Lasing observed in NC superparticles(20)

CHAPTER 3 : SYNTHESIS AND CHARACTERIZATION OF NANOCRYSTAL SUPERPARTICLES

3.1. Microfluidic synthesis of nanocrystal superparticles

To make the superparticles, a microfluidic chip was used along with a source-sink emulsion. The Nanocrystals (dispersed in Toluene) would enter the chip through a channel (labeled "Channel-2") and a continuous phase of Sodium Dodecyl Sulfate (SDS) dissolved in Milli-Q water would cut the stream of nanocrystals at a right angle and form droplets. This continuous phase enters via channel-1. The droplets then go into a larger microfluidic channel where a sink emulsion composed of SDS-Milli-Q water and hexadecane is introduced into the stream, which enters from channel-3. The Toluene surrounding the nanocrystals seeps out into the stream and surrounds the hexadecane droplets increasing their size while also decreasing the size of the nanocrystal agglomerates, compressing them into the superparticles(19).

All channels are pressurized at 2000mbar initially until a stable stream of the nanocrystal dispersion is formed. Then, the pressure in channels 2 and 3 are reduced in steps of 200mbar together until it reached a delta of 500-1200mbar compared to channel-1. The combined stream goes out into a twisted coil section that is wound around a copper rod that is maintained at 70°C. This hastens the evaporation of Toluene. Vials are set up at the end of the tube line which has about 2-3mL of the SDS-Milli-Q + hexadecane solution at the bottom to ensure that the superparticles do not break on impact. The final solution is collected in these vials. These vials are then placed on a hot plate until all the toluene has evaporated from the solution.

The particles will usually settle down at the bottom of the vials after a few days on the hot plate. Either that, or they will float to the top (which means the nanocrystal solution might have been too dilute). After all the superparticles seem to have aggregated, take the vials off the hotplate. Now decant the SDS+Milli-Q H₂O+hexadecane solution off, fill

| Parameter | Value |
|--|---------------|
| Concentration of nanocrystal dispersion | 10 %v/v |
| SDS + Milli-Q H ₂ O Concentration | 200mM |
| SDS + Milli-Q H ₂ O : Hexadecane | 90:10 %w/w |
| Pressure set at all channels initially | 2000mbar |
| Pressure set at channels 2 and 3 after stable flow | 500-1200mbar |
| Temperature of copper rod | 70°C |
| Temperature of hot plate | 50°C |
| Centrifuge speed and time | 100g and 5min |

Table 1: Parameters used in the making of superparticles

the rest of the vial with Milli-Q H₂O, and put it in the centrifuge for about 5 minutes at 100g. Keep doing this until there are almost no soapy bubbles left. Then drop cast the particles onto a glass slide and dry it on a hot plate.

3.2. Measuring the optical properties of the superparticles

The CRAIC Spectrophotometer was used to measure the optical properties along with light source for UV excitation and viewing the particles in visible. A blue filter was used to distinguish the particles from the slide surface.

| Parameter | Value |
|------------------------------------|-------------|
| Light source excitation wavelength | 430nm |
| Objective magnification | 10x |
| Spectrophotometer scan area | 26μm x 26μm |
| Integration time | 1000ms |

Table 2: Parameters used in measuring the optical properties of superparticles

The light source is turned off and the aperture is closed and a dark scan is taken. Now the aperture is opened and the light source is turned back on and an empty area of the slide is scanned and used as a reference. Now an area of the slide that has a superparticle is brought to the center of the aperture and the photoluminescence spectrum is taken.

CHAPTER 4 : RESULTS AND DISCUSSION

4.1. Dueling Peaks

In the video game The Legend of Zelda: Breath of the Wild, there is a duet of mountains called *the Dueling Peaks*(2) that looks as shown in Figure 15:



Figure 15: Dueling Peaks mountains in the video game The Legend of Zelda: Breath of the Wild

In the photoluminescence spectrum of most of the superparticles that have been synthesized and characterized in this work, it is a recurring theme that a "dueling peaks"-esque dual-peak spectrum is observed.

4.2. CdTe superparticles

Superparticles have been synthesized using the microfluidic setup, out of CdTe NCs. These superparticles can be seen in Figure 16.

The diameter of the CdTe SPs can be estimated to be approximately $8\mu\text{m}$ from the optical micrographs.

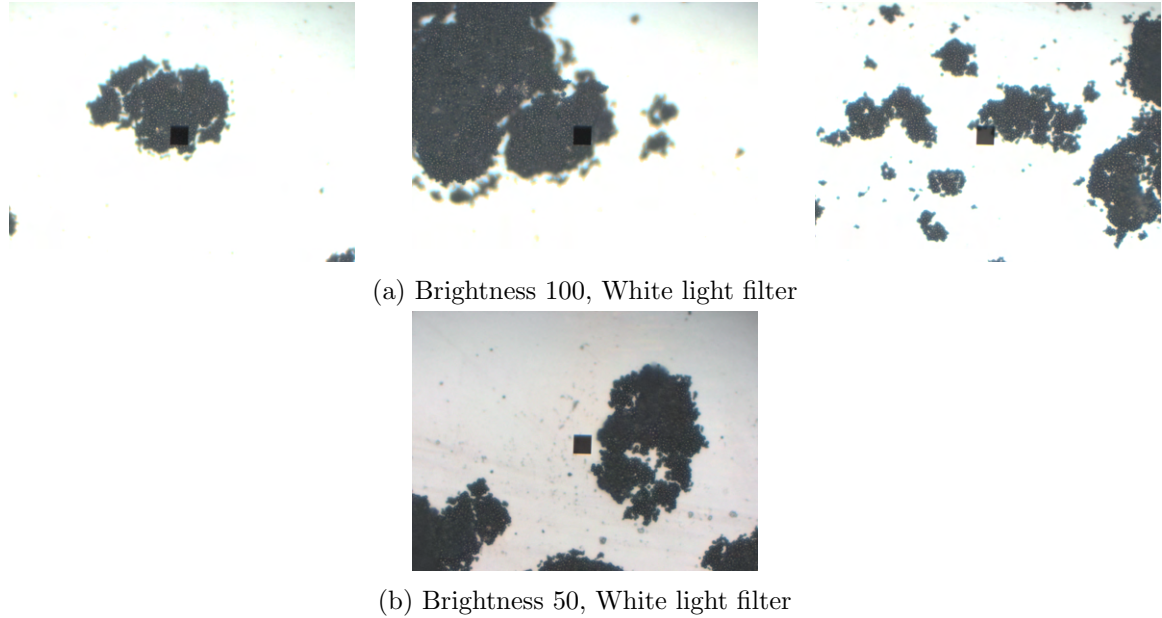


Figure 16: CdTe superparticles optical micrographs

4.3. CdSe superparticles

Superparticles have been synthesized using the microfluidic setup, out of CdSe NCs. These NCs have an absorbance peak at around 550nm. These superparticles, along with their Photoluminescence spectra can be seen in Figure 18. Given in Figure 17 is the absorbance and PL spectra of the NCs used to make the SPs.

An interesting phenomenon can be seen in Figures 18a, 18c, and 18f. From 17, we expect only one peak in the PL of the NCs at around 565.9nm, however, we can see two peaks in the above photoluminescence spectra. One peak is close to the expected value of 565.9nm, while the other is at around 603-609nm. This "dueling peaks" phenomenon could be due to a F.R.E.T-like interaction between neighboring SPs, where a critical number of neighbors gives rise to one peak over the other. It could also be that the spacegroup of the superlattice formed by the NCs is different in different SPs which could have given rise to different peaks. The expected peak is also slightly redshifted or blueshifted in Figures 18a, 18c, and 18f, and Figures 18b and 18d respectively. In Figure 18a, the peak appears to be jagged, which

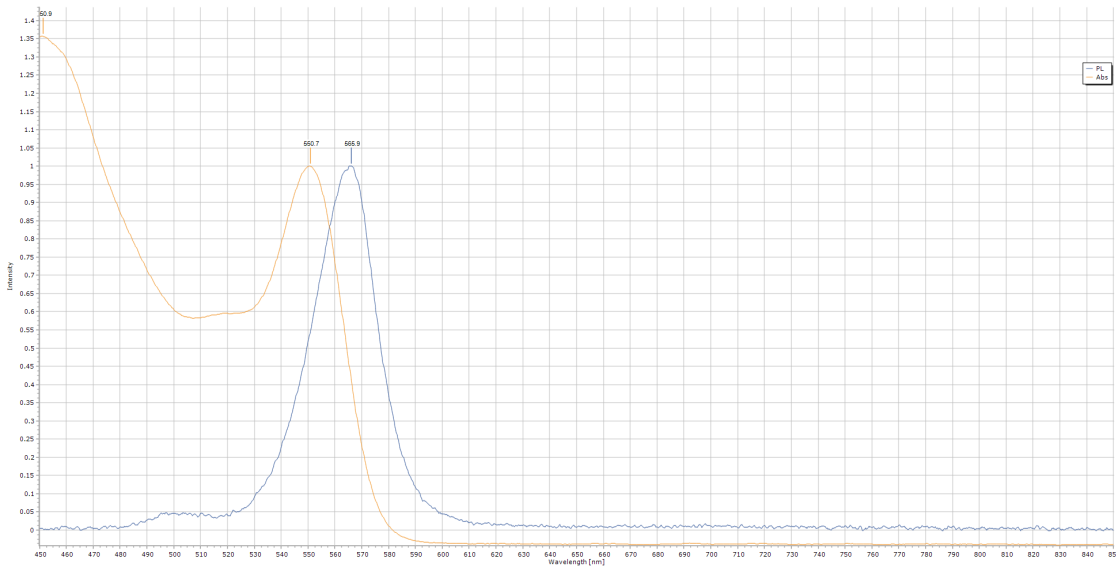
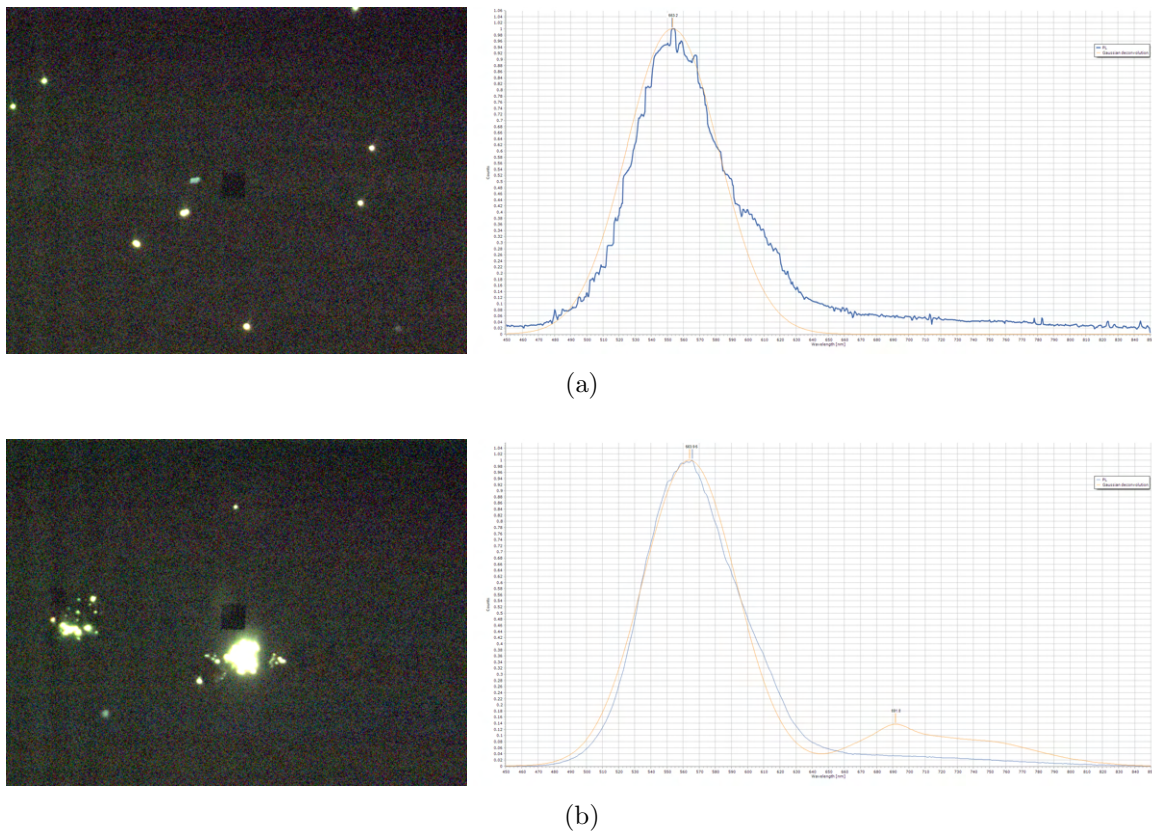


Figure 17: PL and Absorbance Spectra of CdSe [550nm] NCs.



(b)

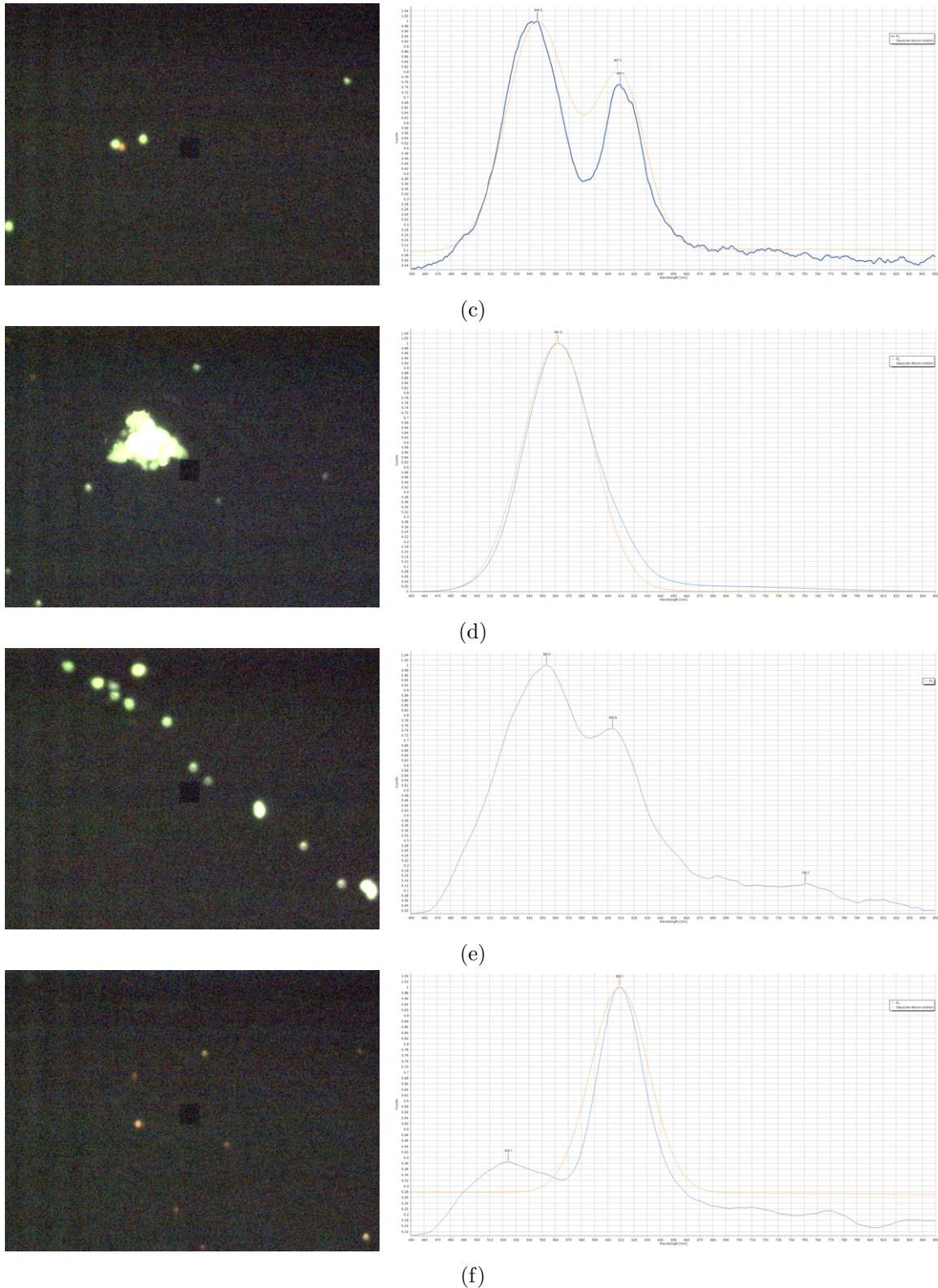


Figure 18: CdSe [550nm] superparticles optical micrographs and corresponding PL spectra at various locations on the substrate.

might be attributed to whispering gallery modes of the SP, but more characterization is necessary to be certain. Perhaps that SP was of the right diameter for WGMs to arise.

When another batch of SPs was synthesized a few weeks later, the dueling peaks were not observed as can be seen in Figure ???. It was not immediately clear as to what the difference in the synthesis method was in both cases, except for maybe the fact that the first batch was made immediately after SPs were made from CdSe/CdS core-shell NCs, which had a PL peak at roughly where the second peak was visible in the spectrum. So it might be that some NCs from the core-shell sample were still stuck to the walls of the tubes used to make the SPs and this is what may have given rise to the second peak. To test this hypothesis, core-shell NCs were purposefully mixed with core NCs to make SPs, the results of which will be discussed in the next section.

However, it is surprising that the dueling peaks re-appear when a different sample of CdSe NCs is used. One thing in common between this batch of SPs and the very first batch was that both were made when the microfluidic chip used to make the SPs was on the verge of being fully clogged due to continued use. This supports the hypothesis that it might be a change in the superlattice configuration and polydispersity of SPs, but further characterization is needed to ascertain this.

4.4. CdSe + CdSe/CdS superparticles

To test the hypothesis that a combination of core and core-shell NCs gave rise to the second peak, the two species were intentionally mixed in different ratios and the PL was measured for the resulting SPs. The core sample used was the same one used in the very first batch, i.e. CdSe [550nm]. The Absorbance and PL of the core-shell NCs used is given in Figure 17. The larger Stokes shift relative to the core NCs is readily apparent.

Two peaks are observed in both concentrations of hetero-superparticles, but there is very little overlap between the peaks compared to the core. This suggests that the core-shell NCs may not be the reason for the dueling peaks observed in earlier samples of core NC SPs. Further study is required to fully determine this, however.

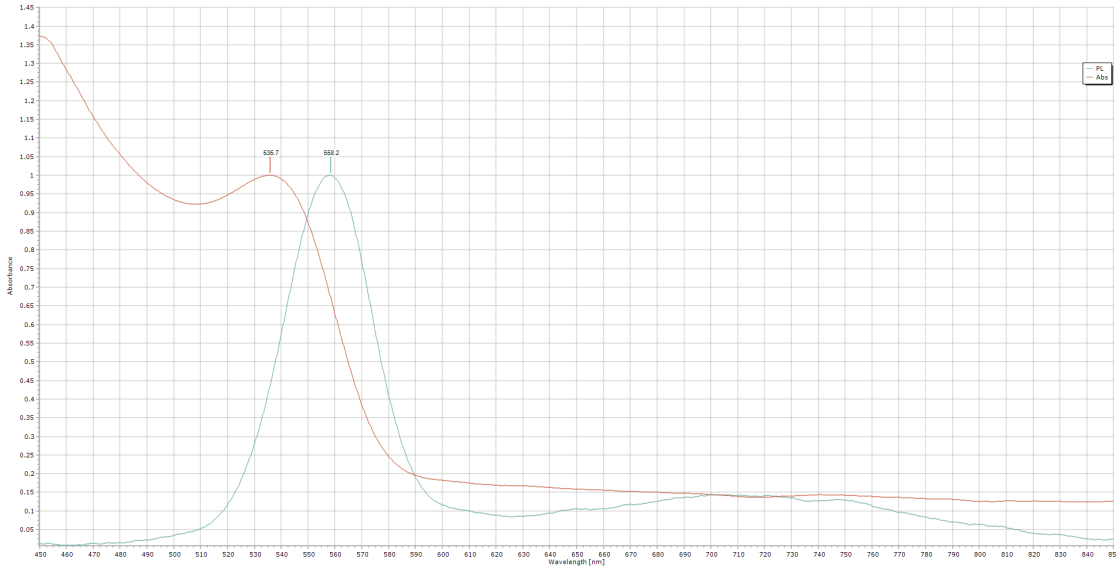
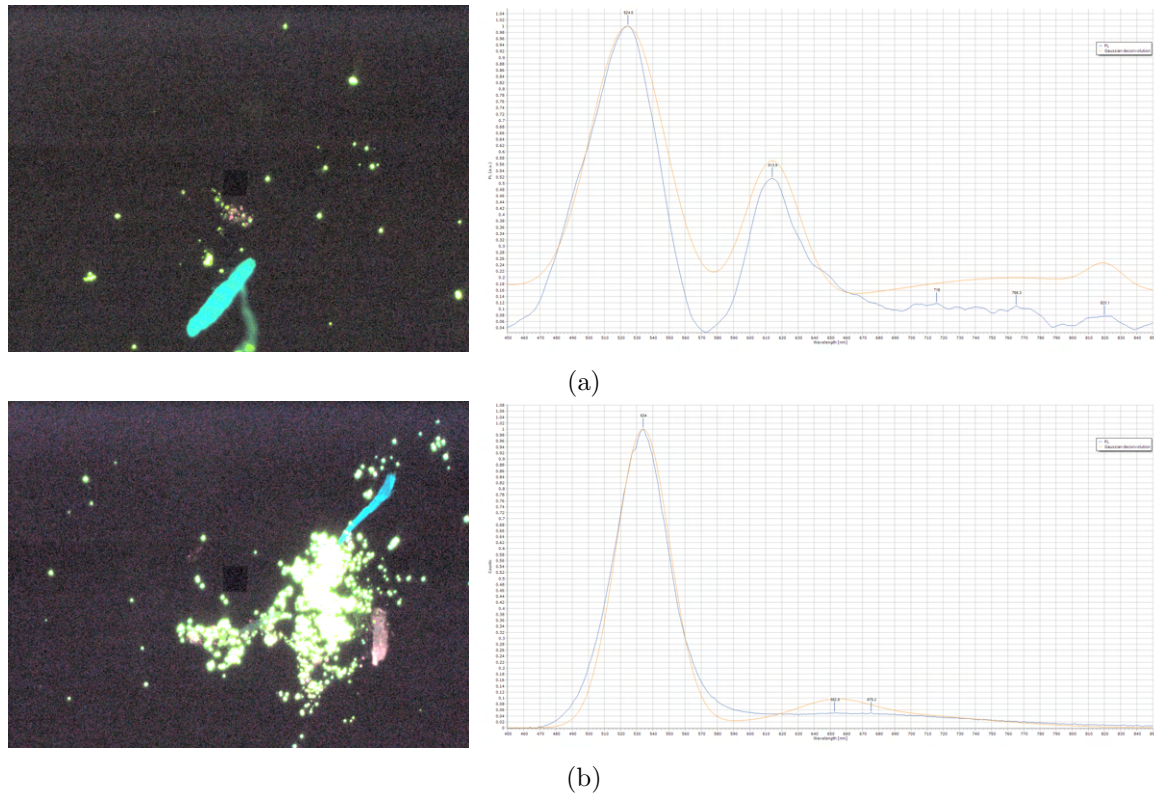


Figure 19: PL and Absorbance Spectra of CdSe [536nm] NCs.



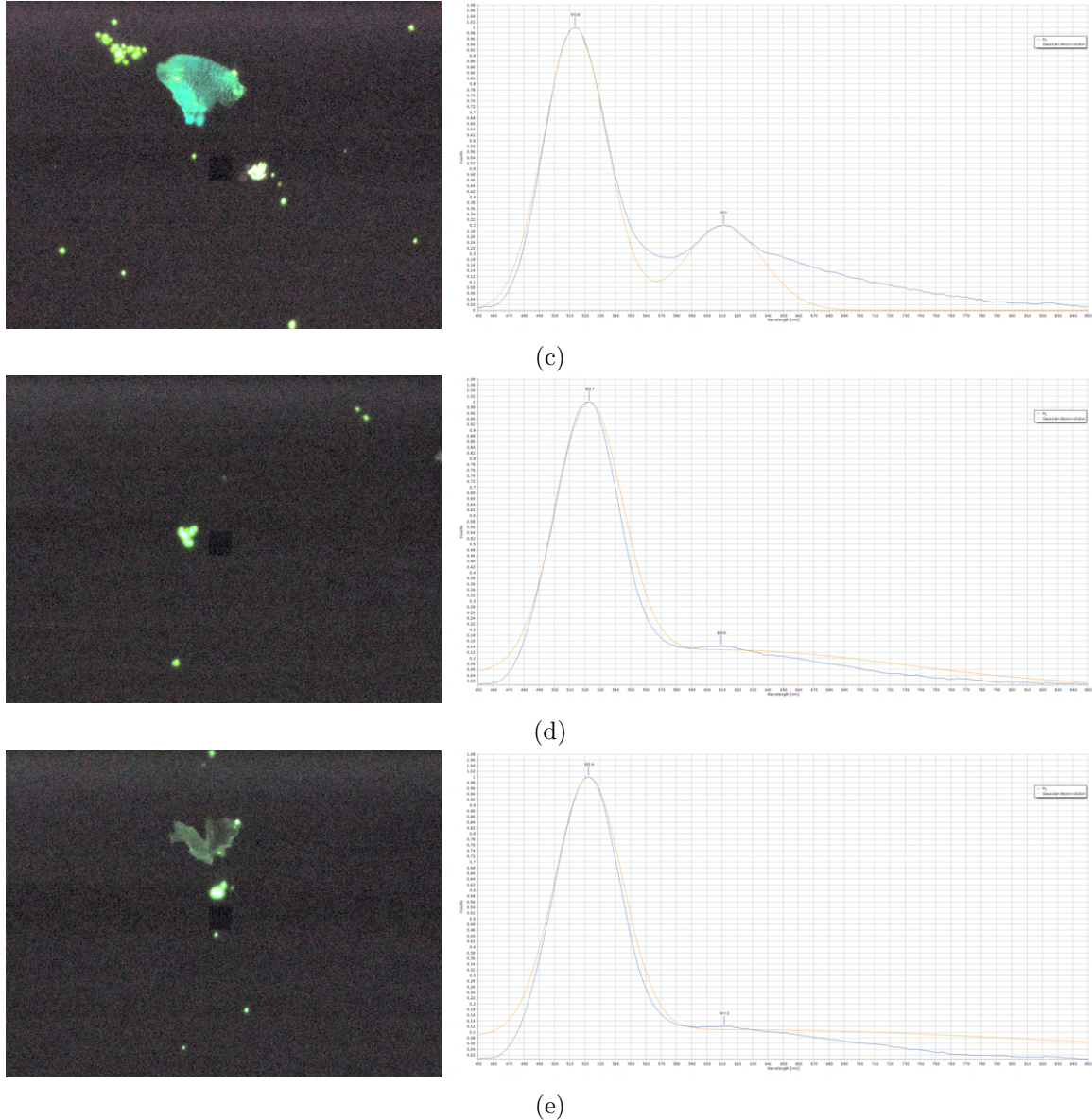


Figure 20: CdSe [536nm] superparticles optical micrographs and corresponding PL spectra at various locations on the substrate. The second peak re-emerges as well as a significant population of red-emitting SPs.

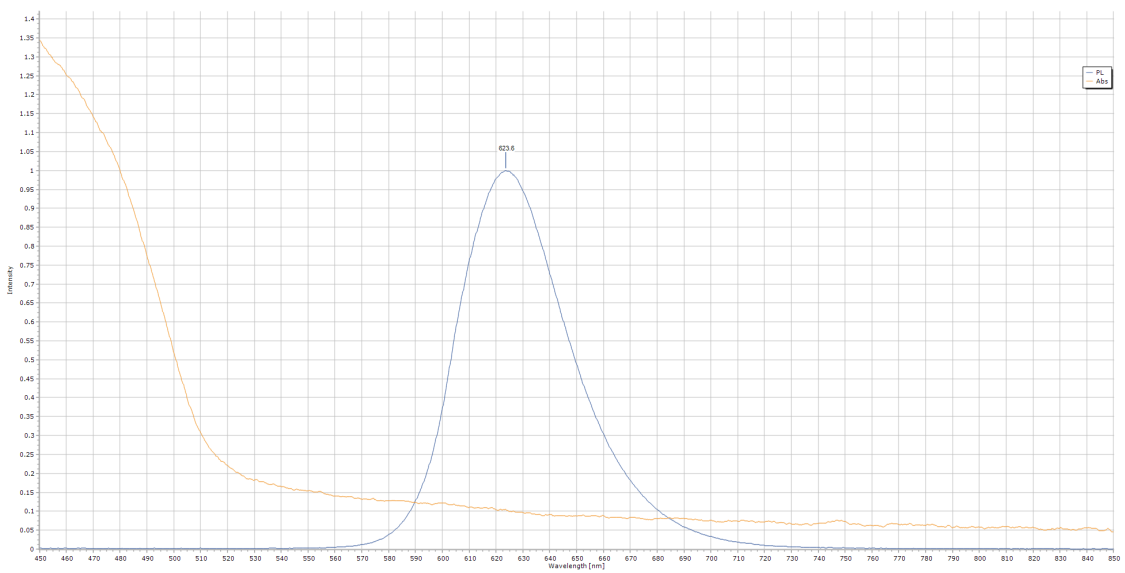


Figure 21: PL and Absorbance Spectra of CdSe/CdS core-shell NCs used to make SPs.

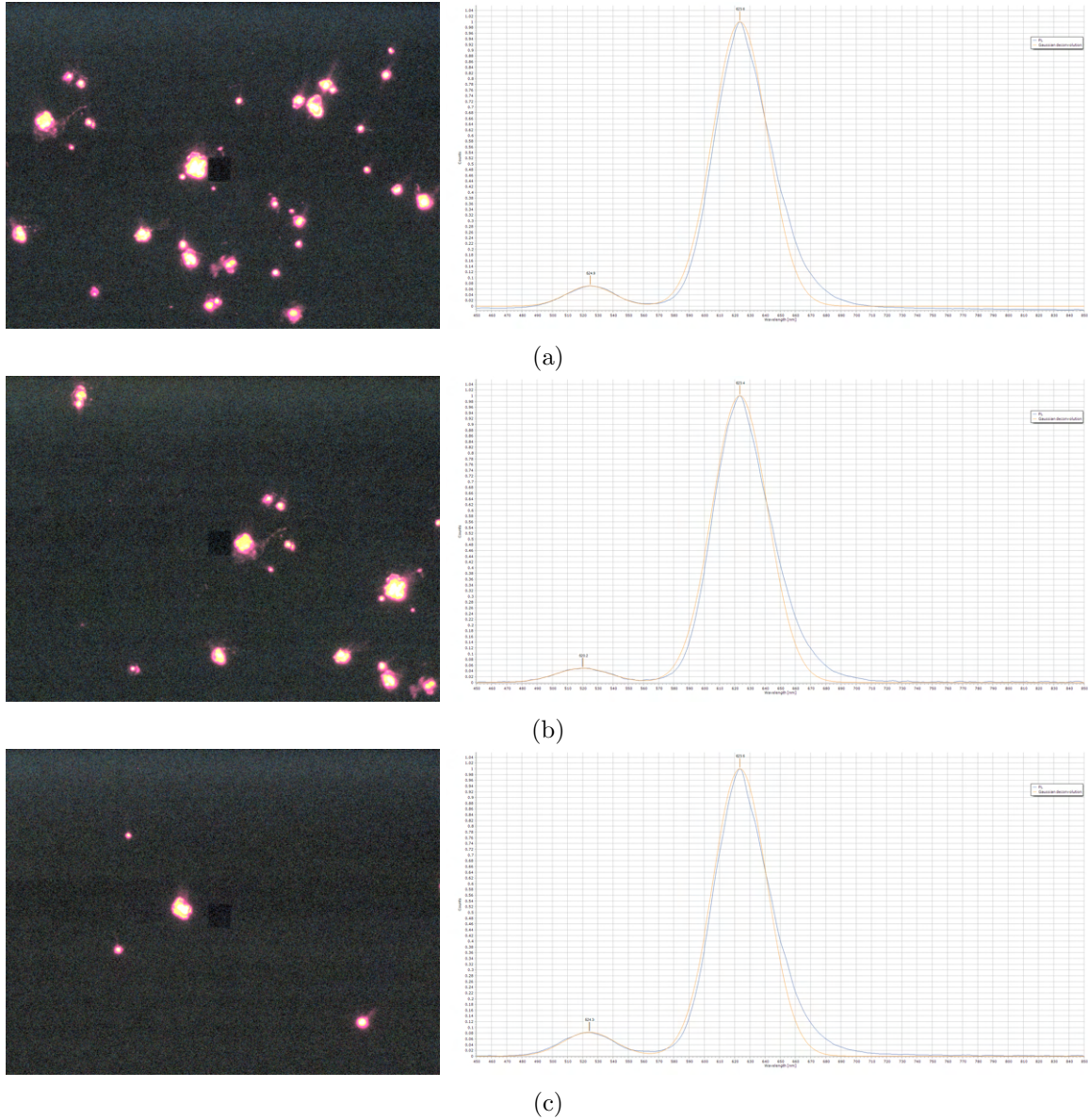
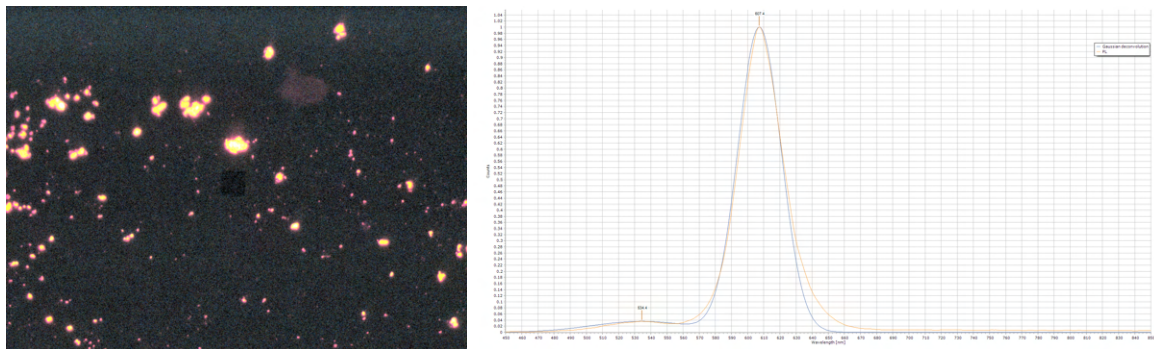
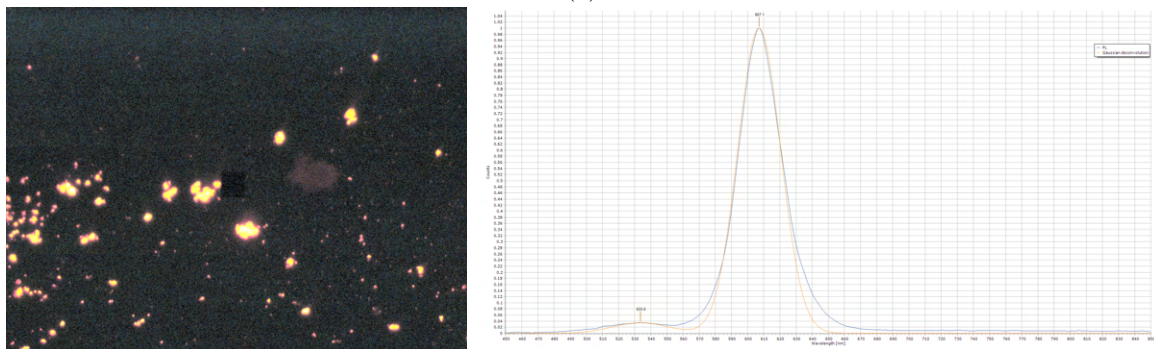


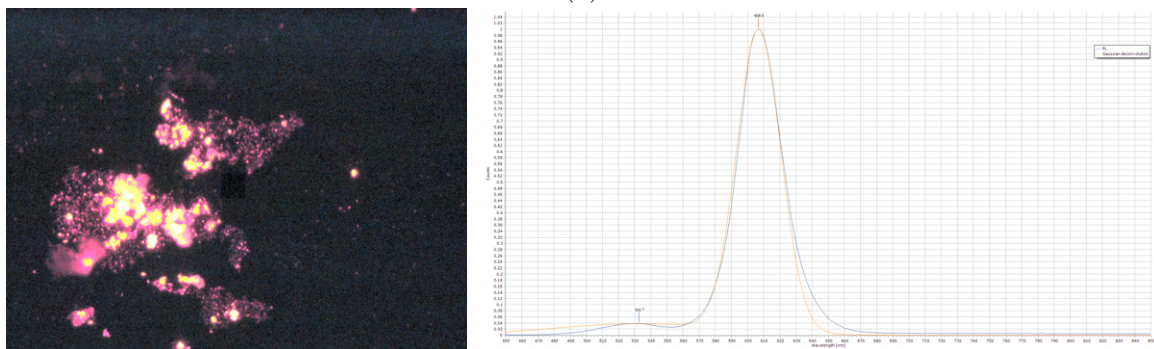
Figure 22: $\text{CdSe}_{0.25}\text{CdSe}/\text{CdS}_{0.75}$ superparticles optical micrographs and corresponding PL spectra at various locations on the substrate. Two peaks are observed.



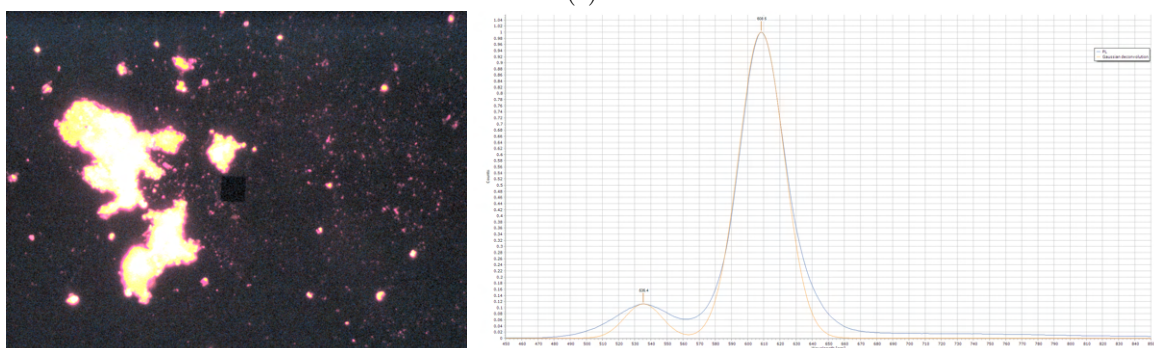
(a)



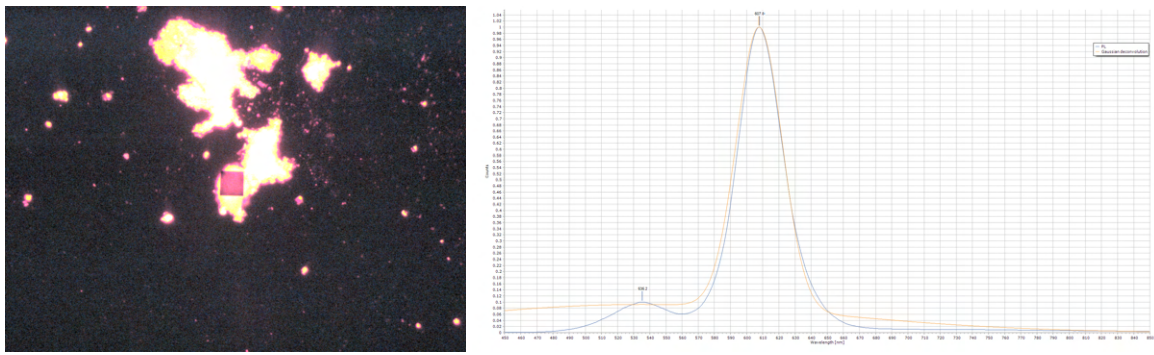
(b)



(c)



(d)



(e)

Figure 23: $\text{CdSe}_{0.5}\text{CdSe}/\text{CdS}_{0.5}$ superparticles optical micrographs and corresponding PL spectra at various locations on the substrate. Two peaks are observed.

CHAPTER 5 : FURTHER WORK

5.1. Solving the mystery of the dueling peaks

As we have seen there are two peaks in the PL of pure CdSe NC SPs. The exact reason for this is still a mystery. A few hypotheses and observations are given below:

- There might be two stable superlattice configurations, one corresponding to each peak. The clogged chips most likely contributed to a different superlattice formation, if there is a difference.
- Number of neighbor SPs might have a role, but given the modal nature of the peaks as opposed to being continuous, this might have less of an effect compared to the above.
- Addition of core-shell species did give rise to two peaks, but the peaks seem to be independent versus there being an overlap in the case of the core NC SPs. This might not be the reason.

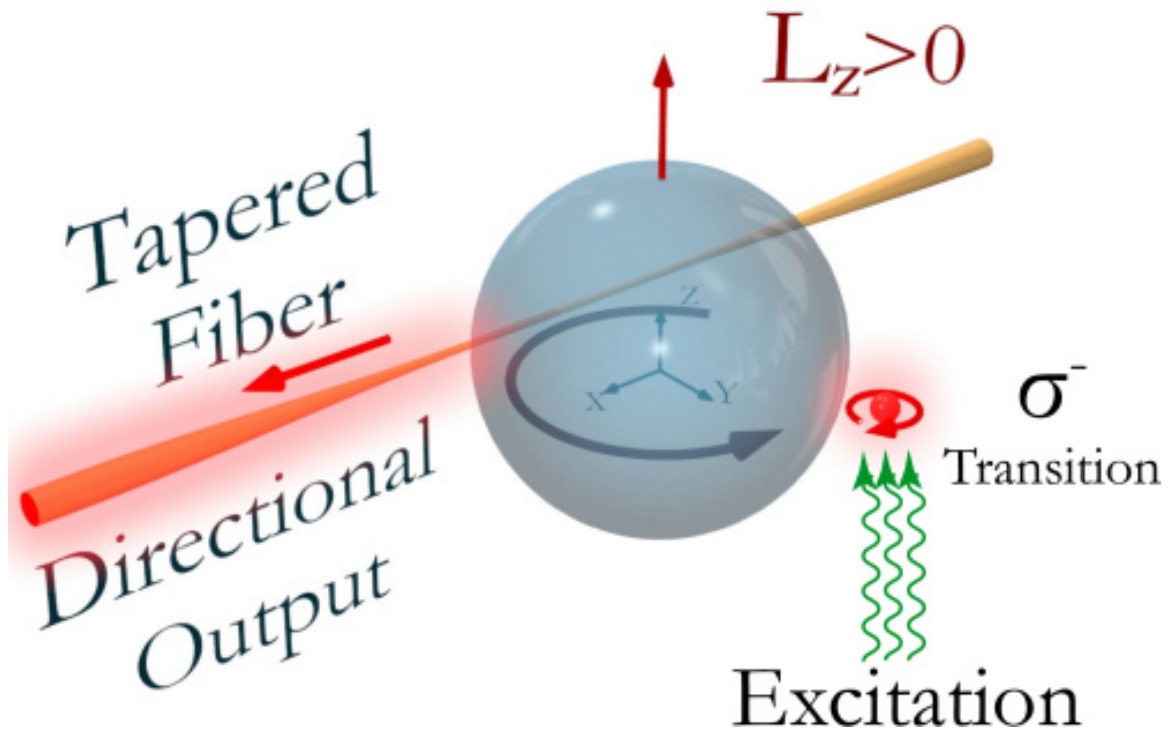


Figure 24

5.2. Solution-Processed twisted light laser

Coupling between the whispering gallery modes of the superparticle and a Zeeman transition in the individual nanocrystals can potentially be used to generate light with orbital angular momentum which can be tuned by changing the ratio of the size of the superparticle and/or the extent of Zeeman splitting (14). The red source shown in Figure 24 behaves like a nanocrystal on the surface of the superparticle. Using Mn^{2+} -doped CdSe or magnetic perovskites could be a great way to make solution-processed OAM lasers.

APPENDIX

A.1. Optical characterization methodology for Nanocrystals

The optical properties of the nanocrystals was measured using an Ocean optics Spectrometer, with a Deuterium-Tungsten Halogen lamp that covers UV, Visible and NIR wavelength range for illumination.

A.1.1. Absorption

2mL of Toluene was taken in a cuvette and placed in the cuvette holder which housed optical fibers to illuminate the sample and measure the light on the other side of the sample. The spectrum is measured as a reference. The optical fibers was blocked from outside light and a dark scan was taken. 2mL of the nanocrystals dispersed in Toluene was taken in another cuvette and the absorption spectrum was measured.

A.1.2. Photoluminescence

The optical fibers were blocked from outside light and a dark scan was taken. 2mL of the nanocrystals dispersed in Toluene was taken in another cuvette and put in the cuvette holder. A 430nm UV laser was used to excite the sample. The photoluminescence spectrum was measured.

BIBLIOGRAPHY

- [1] Absorbance, pl, and stokes shift. <https://www.lateralflows.com/quantum-dots/>.
- [2] Dueling peaks, from the legend of zelda wiki. <https://www.zeldadungeon.net/breath-of-the-wild-walkthrough/dueling-peaks/>.
- [3] Quantum confinement. https://commons.wikimedia.org/wiki/File:Quantum_confinement_1.png.
- [4] Quantum confinement effects on absorption spectrum line broadening of cdse artificial atoms. 14(13).
- [5] Size dependence on absorbance and photoluminescence spectra. https://chem.libretexts.org/Bookshelves/Analytical_Chemistry/Physical_Methods_in_Chemistry_and_Nano_Science_\%28Barron\%29/08\%3A_Structure_at_the_Nano_Scale/8.05\%3A_Spectroscopic_Characterization_of_Nanoparticles#mjax-eqn-10.
- [6] Surface states. https://en.wikipedia.org/wiki/Surface_states.
- [7] High-speed and high-contrast two-channel all-optical modulator based on solution-processed cdse/zns quantum dots. 12(1):12778, Jan 2022.
- [8] David R. Baker and Prashant V. Kamat. Tuning the emission of cdse quantum dots by controlled trap enhancement. *Langmuir*, 26(13):11272–11276, 2010. PMID: 20373780.
- [9] Clemens Burda, Xiaobo Chen, Radha Narayanan, and Mostafa A. El-Sayed. Chemistry and properties of nanocrystals of different shapes. *Chemical Reviews*, 105(4):1025–1102, 2005. PMID: 15826010.
- [10] S. Chandramohan, Beo Deul Ryu, Hyun Kyu Kim, Chang-Hee Hong, and Eun-Kyung Suh. Trap-state-assisted white light emission from a cdse nanocrystal integrated hybrid light-emitting diode. *Opt. Lett.*, 36(6):802–804, Mar 2011.
- [11] Kenny F Chou and Allison M Dennis. Förster resonance energy transfer between quantum dot donors and quantum dot acceptors. *Sensors (Basel)*, 15(6):13288–13325, June 2015.
- [12] F. Pelayo García de Arquer, Dmitri V. Talapin, Victor I. Klimov, Yasuhiko Arakawa, Manfred Bayer, and Edward H. Sargent. Semiconductor quantum dots: Technological progress and future challenges. *Science*, 373(6555):eaaz8541, 2021.
- [13] Gregory Kalyuzhny and Royce W. Murray. Ligand effects on optical properties of cdse nanocrystals. *The Journal of Physical Chemistry B*, 109(15):7012–7021, 2005. PMID: 16851797.

- [14] Farhad Khosravi, Cristian L. Cortes, and Zubin Jacob. Spin photonics in 3d whispering gallery mode resonators. *Opt. Express*, 27(11):15846–15855, May 2019.
- [15] Sudhir Kumar, Jakub Jagielski, Tommaso Marcato, Simon F Solari, and Chih-Jen Shih. Understanding the ligand effects on photophysical, optical, and electroluminescent characteristics of hybrid lead halide perovskite nanocrystal solids. *J Phys Chem Lett*, 10(24):7560–7567, December 2019.
- [16] Cong Li, Xiaoyun Qin, Zhenghao Zhang, Yujia Lv, Shengwei Zhang, Yijie Fan, Shiyuan Liang, Bowen Guo, Zhou Li, Yan Liu, and Dan Luo. Structure-activity collective properties underlying self-assembled superstructures. *Nano Today*, 42:101354, 2022.
- [17] Jaehoon Lim, Wan Ki Bae, Jeonghun Kwak, Seonghoon Lee, Changhee Lee, and Kookheon Char. Perspective on synthesis, device structures, and printing processes for quantum dot displays. *Optical Materials Express*, 2:594–628, 05 2012.
- [18] Emanuele Marino, Harshit Bharti, Jun Xu, Cherie R. Kagan, and Christopher B. Murray. Nanocrystal superparticles with whispering-gallery modes tunable through chemical and optical triggers. *Nano Letters*, 22(12):4765–4773, 2022. PMID: 35649039.
- [19] Emanuele Marino, Sjoerd W. van Dongen, Steven J. Neuhaus, Weixingyue Li, Austin W. Keller, Cherie R. Kagan, Thomas E. Kodger, and Christopher B. Murray. Monodisperse nanocrystal superparticles through a source–sink emulsion system. *Chemistry of Materials*, 34(6):2779–2789, 2022.
- [20] Federico Montanarella, Darius Urbonas, Luke Chadwick, Pepijn G. Moerman, Patrick J. Baesjou, Rainer F. Mahrt, Alfons van Blaaderen, Thilo Stöferle, and Daniel Vanmaekelbergh. Lasing supraparticles self-assembled from nanocrystals. *ACS Nano*, 12(12):12788–12794, 2018. PMID: 30540430.
- [21] C. B. Murray, C. R. Kagan, and M. G. Bawendi. Synthesis and characterization of monodisperse nanocrystals and close-packed nanocrystal assemblies. *Annual Review of Materials Science*, 30(1):545–610, 2000.
- [22] Kamalpreet Singh and Oleksandr Voznyy. It’s a trap! fused quantum dots are undesired defects in thin-film solar cells. *Chem*, 5(7):1692–1694, 2019.
- [23] M.S. Skolnick and D.J. Mowbray. Self-assembled semiconductor quantum dots: Fundamental physics and device applications. *Annual Review of Materials Research*, 34(1):181–218, 2004.
- [24] Damon A. Wheeler and Jin Z. Zhang. Exciton dynamics in semiconductor nanocrystals. *Advanced Materials*, 25(21):2878–2896, 2013.